

Limits of In(Ga)As/GaAs quantum dot growth

A. Lenz^{*1}, H. Eisele^{1,2}, R. Timm¹, L. Ivanova¹, R. L. Sellin¹, H.-Y. Liu³, M. Hopkinson³, U. W. Pohl¹, D. Bimberg¹, and M. Dähne¹

¹ Institut für Festkörperphysik, Technische Universität Berlin, 10623 Berlin, Germany

² Department of Physics, University of Texas at Austin, Austin, Texas 78712, USA

³ Department of Electronic and Electrical Engineering, University of Sheffield, Sheffield S1 3JD, UK

Received 23 April 2008, accepted 27 September 2008

Published online 14 January 2009

PACS 68.37.Ef, 68.65.Hb, 81.07.Ta, 81.15.Gh, 81.15.Hi, 81.16.Dn

* Corresponding author: e-mail alenz@physik.tu-berlin.de, Phone: +49-30-31422057, Fax: +49-30-31426181

For the formation of large In(Ga)As/GaAs quantum dots, aiming at emission wavelengths of 1.3 μm , strategies like the use of strain reducing diluted InGaAs capping layers or the growth of InAs quantum dots embedded in InGaAs quantum wells are very promising. Using cross-sectional scanning tunneling microscopy we observed for both concepts an increased

quantum dot size, but also defective quantum dots, characterized by a material hole or so-called nanovoid. The process of such nanovoid formation is investigated in detail, considering the strain and the limited growth kinetics during capping. The existence of nanovoids impressively shows the limitations of growing larger and thus more strained quantum dots.

© 2009 WILEY-VCH Verlag GmbH & Co. KGaA, Weinheim

1 Introduction In order to reach the technologically important emission wavelength of 1.3 μm for GaAs-based semiconductor lasers or optical amplifiers [1, 2] the overgrowth of In(Ga)As quantum dots with a diluted InGaAs layer [3, 4] or the growth of InAs quantum dots within an InGaAs quantum well (DWELL) [5–8] are promising methods. Here we present a cross-sectional scanning tunneling microscopy (XSTM) study of such In(Ga)As/GaAs quantum dot samples grown with metal-organic chemical vapor deposition (MOCVD) and molecular beam epitaxy (MBE). In both cases the quantum dot size increases as compared with conventional In(Ga)As quantum dots, but additionally several quantum dots contain a material hole and hence will not contribute to the lasing process, degrading the efficiency of the device. The similarities and differences between these quantum dots grown with different strategies using different epitaxial methods are investigated. We obtain the mechanisms which are responsible for the formation of these defective quantum dots, representing limits of larger quantum dot growth.

2 Experimental details The laser diode structure labelled sample A contains a strain reducing diluted InGaAs

layer on top of the quantum dots and was grown using MOCVD. Here, 3–5 ML $\text{In}_{0.80}\text{Ga}_{0.20}\text{As}$ were deposited at 500 °C with a growth rate of 1 ML/s, followed by a 60 s long growth interruption for quantum dot formation. Afterwards the quantum dots were covered by 3 nm $\text{In}_{0.10}\text{Ga}_{0.90}\text{As}$ and 2–3 nm GaAs. During the subsequent deposition of 3–4 nm GaAs, the temperature was raised to 600 °C. Then a further growth interruption of 10 min was introduced in order to flatten the growth surface and to anneal defects [9, 10]. Finally the quantum dot structures were capped by 20 nm GaAs at a very fast growth rate of 21 ML/s.

Sample B contains two different MBE-grown structures, named DWELL 1 and DWELL 2, differing only in the thickness of the low temperature GaAs cap layer deposited prior to a growth interruption. The DWELL sequence starts with 2 nm $\text{In}_{0.15}\text{Ga}_{0.85}\text{As}$ and 2.8 ML InAs quantum dot material, followed by a 10 s growth interruption for quantum dot formation, and finally 6 nm $\text{In}_{0.15}\text{Ga}_{0.85}\text{As}$. After this DWELL growth at 510 °C the nanostructures are capped, in the case of DWELL 1 with 10 nm GaAs followed by a 2 min long growth interruption and further GaAs cap growth at 580 °C. In the case of

DWELL 2 the thickness of the GaAs cap layer deposited prior to the growth interruption and temperature increase is only 2 nm instead of 10 nm.

3 Results Conventional quantum dots observed in samples A and B are shown in Fig. 1. The lateral sizes of quantum dots at sample A amount to about 10–25 nm and their heights to about 5 nm, while the quantum dots at sample B in DWELL 1 and DWELL 2 have lateral sizes amounting to 30 nm and 20–25 nm and heights of about 6–9 nm and 5–7 nm, respectively. The shapes of conventional quantum dots are indicated by the solid contour lines, while the borderlines of the diluted InGaAs layer and the InGaAs DWELL region are indicated by the dotted ones. It can be nicely seen that the highest indium concentration is found in the quantum dot center close to the truncated quantum dot apex [11].

Besides these conventional quantum dots also defective quantum dots or so-called nanovoids are found in sample A and in DWELL 1 of sample B with percentages of 40% and 30%, respectively. Representative examples of such quantum dots containing nanovoids are shown in Fig. 2. The quantum dots containing nanovoids are generally larger than the conventional quantum dots. The nanovoid size of sample A (Fig. 2a, b) varies laterally between 3 nm and 10 nm and amounts in growth direction to about 3 nm. Furthermore single indium atoms are clearly observed above the nanovoids of sample A, forming a sec-

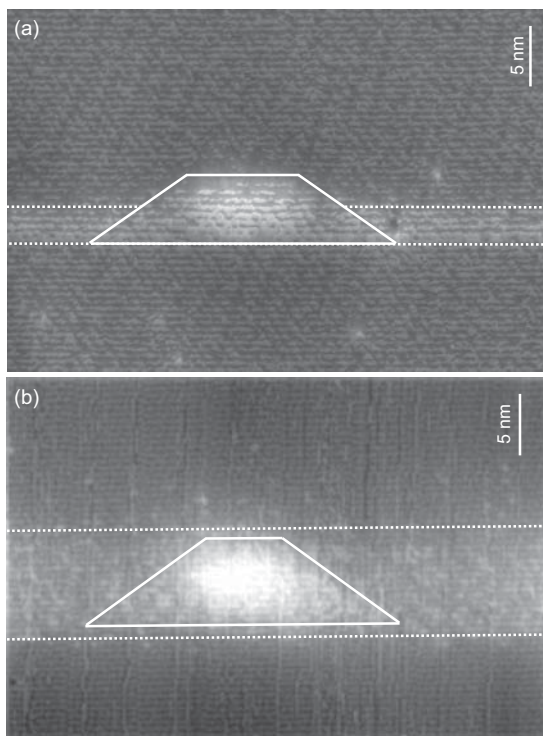


Figure 1 Conventional quantum dots observed (a) in sample A and (b) in DWELL 1 of sample B.

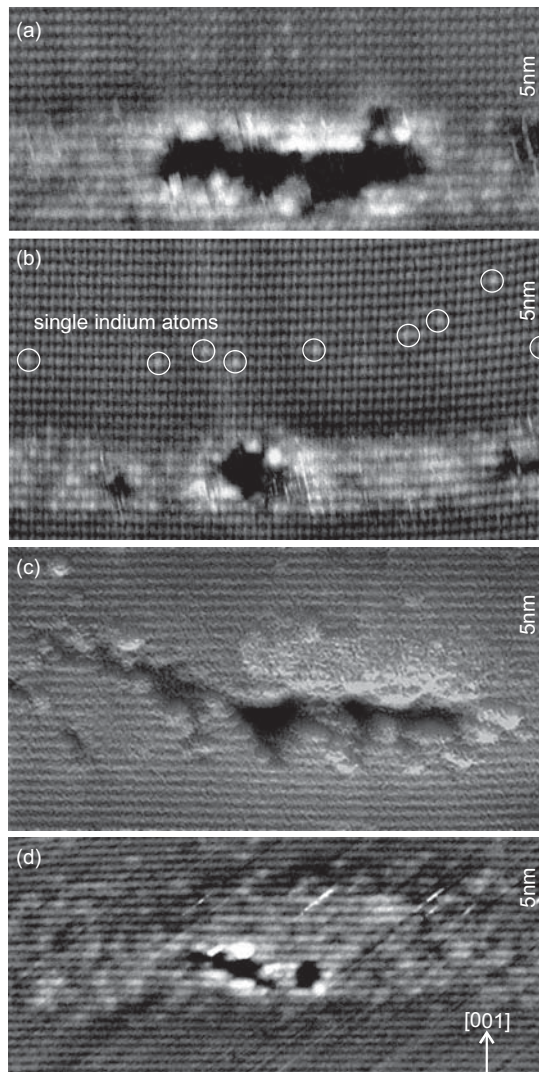


Figure 2 Nanovoids observed (a), (b) in sample A and (c), (d) in DWELL 1 of sample B.

ond wetting layer [12]. In the case of DWELL 1 of sample B (Fig. 2c, d), the sizes of the nanovoids are even larger, varying between 5 nm and 20 nm laterally and between 1 nm and 5 nm along growth direction. The nanovoids in sample A are located at the position of the formerly highest indium concentration of the quantum dots, while the nanovoid position in sample B varies between the quantum dot center and its edges, and their shape is further found to be more elongated.

4 Discussion In the following the formation process of the nanovoids will be discussed. The schematic growth model for the nanovoids of the MOCVD grown sample A [12] is shown in Fig. 3 and will be described from top to bottom. The largest quantum dots of sample A are capped by only a very thin GaAs layer prior to a 10 minutes long growth interruption (1). Hence, the strain

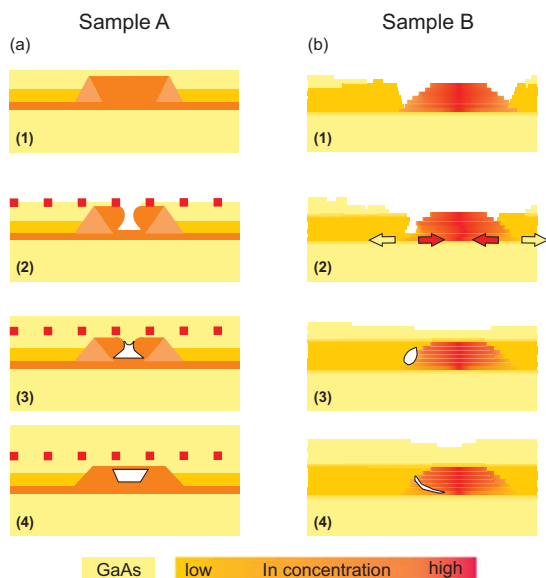


Figure 3 (online colour at: www.pss-b.com) Schematic model of the nanovoid formation (a) for sample A and (b) for DWELL 1 of sample B.

of the indium-rich center is so high, that during the growth interruption the quantum dot material can strongly segregate outward also from deeper regions (2) [13]. A second wetting layer is formed at the position where the overgrowth was interrupted, as observed in the XSTM images shown in Fig. 2a, b. The total amount of missing indium atoms in the nanovoids is estimated to 0.3 ML, which is in excellent agreement with the counted amount of indium atoms in the second wetting layer above the nanostructures. If the crater aperture of the nanovoids is narrow enough, the following rather fast overgrowth with GaAs results in a conservation of the nanovoid since surface diffusion of the capping atoms occurs too slowly (3). After closing of the aperture the material hole remains and only a rearrangement of the InAs material in the inner surface of the nanovoid may take place in order to reduce strain and surface energy (4).

Figure 3b presents the evolution of the nanovoids of DWELL 1 of the MBE grown sample B [14], again from top to bottom. The capping process of the large InAs quantum dots starts with 6 nm $\text{In}_{0.15}\text{Ga}_{0.85}\text{As}$ and leads to a flattening of the quantum dot apex. In atomic force microscopy data taken after 2, 4 and 6 nm InGaAs cap layer thickness, the formation of trenches around the quantum dots upon InGaAs deposition is observed (1). This behavior can be attributed to limited surface diffusion kinetics and the large strain energy which would have to be invested when filling the trenches. For the quantum dots in DWELL 1 further 10 nm GaAs are deposited at low temperature. During the GaAs deposition the strain in the InGaAs layer increases considerably, so that many indium atoms segregate into the quantum dot center, while gallium tends to segregate out of the quantum dot, resulting in lar-

ger quantum dots (2). This process is indicated for indium by red arrows (darker in gray scale) and for gallium by yellow (brighter) ones. In addition to this segregation process, some trenches are overgrown forming a nanovoid, since growth kinetic is too slow to fill all trenches (3). During the following growth interruption the 10 nm thick GaAs cap layer preserves the nanovoid, and only a migration of the nanovoid towards the quantum dot center can take place, thereby reducing the local strain energy (4). In the case of DWELL 2 (model not shown here) only a 2 nm thin GaAs cap is deposited prior to the 2 minutes long growth interruption, the latter allowing to fill the trenches by material rearrangement, additionally supported by the faster kinetics due to the increased temperature. Thus conventional quantum dots are observed predominantly for DWELL 2. However, the sizes of the remaining conventional quantum dots are smaller, as already mentioned in Section 3.

From additional investigations of the DWELL sample it was found that lasing at 100 °C occurs at wavelengths of 1.35 μm and 1.29 μm for devices with 10 nm and 2 nm GaAs caps, respectively [15]. This red shift in wavelength for thicker low-temperature GaAs cap layers, indicates an increase in quantum dot size, in agreement with the present structural data. However, room temperature electroluminescence measurements showed a decrease of the intensity in the case of thicker GaAs cap layers and thus a decrease of the sample quality [15]. This decrease can now be well understood taking the present XSTM results of the quantum dots into account, where nanovoids are mainly found for the thicker low temperature capping layer.

The large strain in both samples and the sequence of growth interruptions during capping are playing an important role for the resulting quantum dot structure. Independently of the growth method, the strain and the limited growth kinetics during capping can lead to the formation of nanovoids. Although the formation processes in sample A and B vary in detail, the resulting nanovoid structures are nearly the same. It was found that the introduction of growth interruptions allows intense material rearrangements. In the case of sample A, this results in the observed nanovoid formation due to the subsequent fast overgrowth. In the case of DWELL 2 of sample B, in contrast, the specific growth interruptions avoid the nanovoid formation due to the intense material rearrangement, filling the formerly developed trenches. It should be noted that in an earlier XSTM investigation even the complete dissolution of InAs quantum dots capped with a thin GaAs layer prior to an extended growth interruption was observed, resulting in a two-dimensional InGaAs layer [16]. This again indicates the strong influence of the growth interruptions and the following overgrowth processes.

5 Conclusion The use of diluted InGaAs layers in combination with In(Ga)As quantum dots leads to an increase in the quantum dot size and thus to the desired increase in the emission wavelength. However, the additional

observation of quantum dots containing nanovoids impressively shows the limits of larger quantum dot growth. The reasons for this nanovoid formation are primarily the strain in the system and the limited growth kinetics during capping.

Acknowledgements This work was supported by DFG projects Da 408/12, Sfb 296 TP A4 and A7, and Sfb 787 TP A2 and A4, as well as the SANDiE Network of Excellence of the European Commission.

References

- [1] M. Grundmann (ed.), *Nano-Optoelectronics: Concepts, Physics and Devices*, NanoScience and Technology (Springer, Berlin, 2002).
- [2] V. Shchukin, N. N. Ledentsov, and D. Bimberg, *Epitaxy of Nanostructures* (Springer, Berlin, 2003).
- [3] A. E. Zhukov, A. R. Kovsh, N. A. Maleev, S. S. Mikhrin, V. M. Ustinov, A. F. Tsatsul'nikov, M. V. Maximov, B. V. Volovik, D. A. Bedarev, Yu. M. Shernyakov, P. S. Kop'ev, Z. I. Alferov, N. N. Ledentsov, and D. Bimberg, *Appl. Phys. Lett.* **75**, 1926 (1999).
- [4] F. Guffarth, R. Heitz, A. Schliwa, O. Stier, N. N. Ledentsov, A. R. Kovsh, V. M. Ustinov, and D. Bimberg, *Phys. Rev. B* **64**, 085305 (2001).
- [5] P. G. Eliseev, H. Li, A. Stintz, G. T. Liu, T. C. Newell, K. J. Malloy, and L. F. Lester, *Appl. Phys. Lett.* **77**, 262 (2000).
- [6] Y. Qiu, P. Gogna, S. Forouhar, A. Stintz, and L. F. Lester, *Appl. Phys. Lett.* **79**, 3570 (2001).
- [7] J. X. Chen, U. Oesterle, A. Fiore, R. P. Stanley, M. Illegems, and T. Todaro, *Appl. Phys. Lett.* **79**, 3681 (2001).
- [8] H. Y. Liu, M. Hopkinson, C. N. Harrison, M. J. Steer, R. Frith, I. R. Sellers, D. J. Mowbray, and M. S. Skolnick, *J. Appl. Phys.* **93**, 2931 (2003).
- [9] R. Sellin, F. Heinrichsdorff, Ch. Ribbat, M. Grundmann, U. W. Pohl, and D. Bimberg, *J. Cryst. Growth* **221**, 581 (2000).
- [10] R. L. Sellin, Ch. Ribbat, M. Grundmann, N. N. Ledentsov, and D. Bimberg, *Appl. Phys. Lett.* **78**, 1207 (2001).
- [11] A. Lenz, R. Timm, H. Eisele, Ch. Hennig, S. K. Becker, R. L. Sellin, U. W. Pohl, D. Bimberg, and M. Dähne, *Appl. Phys. Lett.* **81**, 5150 (2002).
- [12] A. Lenz, H. Eisele, R. Timm, S. K. Becker, R. L. Sellin, U. W. Pohl, D. Bimberg, and M. Dähne, *Appl. Phys. Lett.* **85**, 3848 (2004).
- [13] L. G. Wang, P. Kratzer, M. Scheffler, and Q. K. K. Liu, *Appl. Phys. A* **73**, 161 (2001).
- [14] A. Lenz, H. Eisele, R. Timm, L. Ivanova, H.-Y. Liu, M. Hopkinson, U. W. Pohl, and M. Dähne, *Physica E* **40**, 1988 (2008).
- [15] H. Y. Liu, S. L. Liew, T. J. Badcock, D. J. Mowbray, M. S. Skolnick, S. K. Ray, T. L. Choi, K. M. Groom, B. Stevens, F. Hasbullah, C. Y. Jin, M. Hopkinson, and R. A. Hogg, *Appl. Phys. Lett.* **89**, 073113 (2006).
- [16] H. Eisele, A. Lenz, Ch. Hennig, R. Timm, M. Ternes, and M. Dähne, *J. Cryst. Growth* **248**, 322 (2003).